Pharmacological Reports (2022) 74:1315–1325
https://doi.org/10.1007/s43440-022-00398-5

SPECIAL ISSUE: SHORT COMMUNICATION

The Post-COVID Era - Advances and Challenges in Pharmacology

Jacareubin inhibits TLR4-induced lung inflammatory response caused by the RBD domain of SARS-CoV-2 Spike protein

Deisy Segura-Villalobos[1] · Daniela Roa-Velázquez[2] · Dan I. Zavala-Vargas[2] · Jessica G. Filisola-Villaseñor[2] · Jorge Ivan Castillo Arellano[3] · Edgar Morales Ríos[2] · Ricardo Reyes-Chilpa[3] · Claudia González-Espinosa[1]

Received: 10 March 2022 / Revised: 19 July 2022 / Accepted: 22 July 2022 / Published online: 5 August 2022

Abstract

Background COVID-19, the disease caused by SARS-CoV-2 virus infection, has been a major public health problem worldwide in the last 2 years. SARS-CoV-2-dependent activation of innate immune receptors contributes to the strong local and systemic inflammatory reaction associated with rapid disease evolution. The receptor-binding domain (RBD) of Spike (S) viral protein (S-RBD) is essential for virus infection and its interacting molecules in target cells are still under identification. On the other hand, the search for accessible natural molecules with potential therapeutic use has been intense and remains an active field of investigation.

Methods C57BL6/J (control) and Toll-like receptor (TLR) 4-deficient (*Lps del*) mice were nebulized with recombinant S-RBD. Tumor Necrosis Factor-alpha (TNF-α) and Interleukin (IL)-6 production in bronchoalveolar lavages (BALs) was determined by enzyme-linked immunosorbent assay (ELISA). Lung-infiltrating cells recovered in BALs were quantified by hematoxylin–eosin (H&E) stain. In selected groups of animals, the natural compound Jacareubin or dexamethasone were intraperitoneally (ip) administered 2 hours before nebulization.

Results A rapid lung production of TNF-α and IL-6 and cell infiltration was induced by S-RBD nebulization in control but not in *Lps del* mice. Pre-treatment with Jacareubin or dexamethasone prevented S-RBD-induced TNF-α and IL-6 secretion in BALs from control animals.

Conclusions S-RBD domain promotes lung TNF-α and IL-6 production in a TLR4-dependent fashion in C57BL6/J mice. Xanthone Jacareubin possesses potential anti-COVID-19 properties that, together with the previously tested anti-inflammatory activity, safety, and tolerance, make it a valuable drug to be further investigated for the treatment of cytokine production caused by SARS-CoV-2 infection.

Keywords Coronavirus · RBD · Spike protein · TLR4 · Lung inflammation

✉ Ricardo Reyes-Chilpa
chilpa@unam.mx

✉ Claudia González-Espinosa
cgonzal@cinvestav.mx

[1] Departamento de Farmacobiología, Centro de Investigación y de Estudios Avanzados (Cinvestav) Unidad Sede Sur, Calzada de los Tenorios No. 235, Col. Granjas Coapa, Tlalpan, 14330 Mexico City, Mexico

[2] Departamento de Bioquímica, Centro de Investigación y de Estudios Avanzados (Cinvestav), 07360 Mexico City, Mexico

[3] Departamento de Productos Naturales, Instituto de Química, Universidad Nacional Autónoma de México (UNAM), Circuito Exterior s/n. Ciudad Universitaria, Coyoacán, 04510 Mexico City, Mexico

Abbreviations

ACE-2	Angiotensin-converting enzyme
BAL	Bronchoalveolar lavage
COVID-19	Coronavirus disease 2019
EU	Endotoxin unit
IL-1β	Interleukin 1-β
IL-6	Interleukin 6
ip	Intraperitoneally
LAL	Limulus amebocyte lysate
RBD	Receptor-binding domain
S-RBD	RBD of the Spike protein
SARS-CoV-2	Severe acute respiratory syndrome coronavirus 2
S	Spike
TLR4	Toll-like receptor 4

TMPRSS2	Transmembrane serine protease 2
TNF-α	Tumor necrosis factor-α
PAMP	Pathogen-associated molecular pattern.
PRR	Pattern Recognition receptor

Introduction

The ongoing pandemic by Coronavirus disease 2019 (COVID-19) has caused millions of deaths worldwide and has turned into a serious threat to public health. COVID-19 is caused by severe acute respiratory syndrome coronavirus 2 (SARS-CoV-2) and its variants [1]. SARS-CoV-2 is a positive-sense single RNA virus belonging to the *Coronaviridae* family [2]. This virus infects host cells through a mechanism that requires its transmembrane Spike (S) protein, the angiotensin-converting enzyme 2 (ACE-2), and the transmembrane serine protease 2 (TMPRSS2). These last two proteins are highly expressed in pulmonary epithelial cells [3, 4]. S protein is the most important antigen of SARS-CoV-2 and contains two functional subunits: S1, which includes the receptor-binding domain (RBD) that binds to ACE-2, and the subunit S2, required for the fusion of viral and host cell membrane [5]. After infection of host cells, an immune response characterized by the production of inflammatory cytokines and a weak interferon response is triggered [6]. In the most severe cases, patients could develop an uncontrolled pulmonary inflammation leading to an over-release of proinflammatory mediators including tumor necrosis factor-α (TNF-α), interleukin (IL)-6 and IL-1β [6, 7]. Deregulated activation of inflammatory pathways causes a phenomenon known as hypercytokinemia or "cytokine storm", which has been observed in both serum and bronchoalveolar lavages (BALs) of COVID-19 patients [8, 9].

Being excessive inflammation one of the primary events associated with severe cases of COVID-19, there has been increased interest in developing effective therapeutic strategies, including novel natural compounds with anti-inflammatory properties, to help patients coursing severe forms of COVID-19-associated hypercytokinemia. We previously reported the anti-inflammatory properties of Jacareubin, a xanthone molecule found in the heartwood of the American tropical tree *Calophyllum brasiliense*. We demonstrated that Jacareubin inhibits mast cell degranulation in vitro and passive cutaneous anaphylaxis and edema in mice, suggesting that this xanthone could be an efficient antioxidant, antiallergic, and anti-inflammatory molecule [10].

Although it is well known that RBD of the Spike protein (S-RBD) interacts with ACE-2 receptor from the host cells [11], molecular docking studies have shown that S protein also can interact with other receptors, such as Toll-like receptors (TLRs), crucial components of innate immunity specialized in recognizing pathogens or damage-associated molecular patterns. Particularly, these in silico analyses showed that TLR4 binds the S protein of SARS-CoV-2, and this protein–protein interaction is the strongest among all analyzed TLRs [12]. However, the interaction between RBD of S protein and TLR4 has not been investigated in in vivo models that evaluate the lung inflammatory response evoked by nebulization of S-RBD.

Here, we report that nebulized recombinant S-RBD from SARS-CoV-2 induces an early and intense lung inflammation in mice through the activation of TLR4 receptor and that the natural compound Jacareubin prevents S-RBD-induced TNF-α and IL-6 synthesis on mice lungs. Our results add to the notion that TLR4 is a plausible therapeutic target in COVID-19 and suggest that Jacareubin should be further examined as a potential therapeutic agent to prevent the inflammation associated with the disease.

Material and methods

Animals

Eight-to 10-week-old C57BL6/J (C57) and TLR4-deficient male mice (*Lps del)* from The Jackson Laboratory were used (stocks # 000,664 and 007,227, respectively). Mice were maintained in controlled conditions of temperature (22–24° C) and humidity, with free access to food and water. All experimental procedures were approved by the Institutional Committee for the Care and Use of Laboratory Animals (CICUAL, authorization number 74–13). Our procedures also followed the National Institutes of Health (NIH) guidelines for the use and care of laboratory animals.

Reagents

All drugs and chemicals were purchased from Sigma (St. Louis, MO, USA), with the following exceptions: dexamethasone solution for injection (Alin^{R}, 8 mg/2 mL) was from CHINOIN (Mexico City, Mexico); silica gel 70/230 was from Macherey–Nagel (Düren, Germany); silica gel 60 was from Merck (Darmstadt, Germany); sodium chloride (NaCl) and glycerol were from Tecsiquim (México). For the final concentration, all reagents were diluted in sterile saline solution (NaCl 0.9%, PiSA).

Wood collection of Calophyllum brasiliense and isolation of Jacareubin

Identification of *C. brasiliense* Cambess (Clusiaceae) tree was performed at the Selva Lacandona, Chiapas, Mexico, by J.I. Calzada. After collection, a wood sample (00,011-XALw) and a voucher (JIC-3116) were deposited in the

Herbarium and xylotheque "Dr. Faustino Miranda", from the Instituto de Ecología, A.C., at Xalapa, Veracruz, México [10].

Jacareubin was obtained from the methanolic extract (74 g) of chips from the heartwood of the *Calophyllum brasiliense* tree (711 g), by column chromatography silica gel 60, 1 kg with a mobile phase of hexane–ethyl acetate (7:3). A mixture of three xanthones (fractions 138–227) was obtained from the methanolic extract, from which a 6-g sample was separated by column chromatography (1 m height and 5 cm diameter) using 120 g of silica gel 70/230, starting with a mobile phase of hexane and gradually increasing the polarity with ethyl acetate [10].

Jacareubin was eluted with the mobile phase of hexane–ethyl acetate 87:13 (fractions 105–198, 400 mg). The structure and purity of Jacareubin used in this study was determined by ^{1}H-NMR and ^{13}C-NMR (Fig. 1) with a Bruker AVANCE III HD 700 MHz (Cambridge Isotope Laboratories, MA, USA). ^{1}H NMR (700 MHz, deuterated acetone). δ 13.55 (1H, s, OH-1), 8.94 (2H, s, OH-5 & OH-6), 7.62 (1H, d, J = 8.8 Hz, H-8), 6.98 (1H, d, J = 8.8 Hz, H-7), 6.67 (1H, d, J = 10.3 Hz, H-1'), 6.33 (1H, s, H-4), 5.72 (1H, d, J = 10.3 Hz, H-2'), 1.47 (6H, s, CH_3-4' & CH_3-5'). ^{13}C NMR (175 MHz, deuterated acetone) δ 181.30 (C-9), 161.08 (C-1), 158.67 (C-3), 157.85 (C-4a), 152.25 (C-6), 146.87 (C-5a), 133.23 (C-5), 128.65 (C-2'), 117.47 (C-8), 115.79 (C-7), 114.71 (C-8a), 113.83 (C-1'), 105.21 (C-2), 103.55 (C-9a), 95.52 (C-4), 78.96 (C-3') and 28.48 (C-4' & C-5'). Jacareubin was analyzed by High-Performance Liquid Chromatography (HPLC–UV) as described previously [10]. Finally, mass spectrometry of the batch used in this study was performed by Direct Analysis in Real-Time (DART) m/z (%): 327 $M^{+}+1$ (100); 326 (7) M+, in an AccuTOF JMS-T100LC equipment (Tokyo, Japan), and the purity was > 99% (Figure S1).

Recombinant S-RBD of SARS-CoV-2 purification

The S-RBD gene was synthesized by Synbio Technologies with codon optimization for *Escherichia coli* production. This gene was sub-cloned into a modified pRSET-A plasmid [13] and the sequence was optimized for better solubility by deleting amino acid residues from the N-and C-term (RBD-NTCT). The final construction was expressed in SoluBL21 (DE3) *Escherichia coli* strain (Genlantis, USA) and purified as described [14]. The

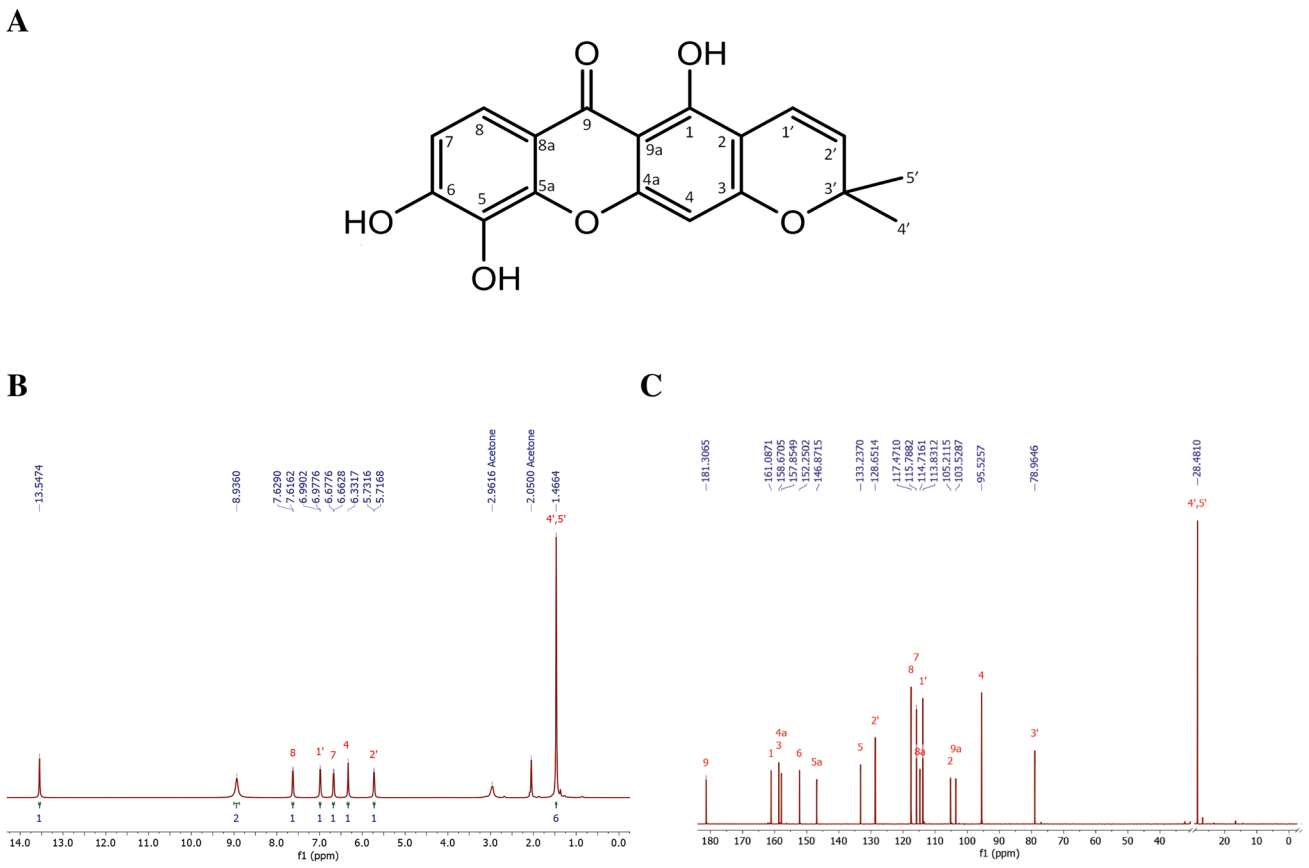

Fig. 1 Structure of Jacareubin **A** and its ^{1}H-NMR (700 MHz) **B** and ^{13}C-NMR (175 MHz) **C** spectra

purified S-RBD was stored in refolding buffer with the following composition in mM: 20 Tris–HCl pH 8.0, 100 NaCl, 0.4 oxidized glutathione, 0.2 reduced glutathione, 1 phenylmethanesulfonyl fluoride (PMSF), 100 arginine, and 5% glycerol. S-RBD was maintained at -70 ºC for later use. Figure 2A shows the final step of the purification process of the S-RBD domain, where the purity of the protein was confirmed by SDS-PAGE electrophoresis (Fig. 2B). For all the experiments, a mixture of fractions a, b, and c was utilized.

In addition, endotoxin concentration was measured in three different samples of the stocks of S-RBD that were used in this study using the ToxinSensor™ Chromogenic LAL Endotoxin Assay Kit (GeneScript, USA; cat. number: L00350), following the manufacturer's instructions. Less than 3.24 EU/mL were detected in the S-RBD stock samples analyzed. Since, for nebulization experiments, those stocks were diluted 1:5 with endotoxin-free saline solution, the final concentration of endotoxin in the nebulization solution was less than 0.648 EU/mL, which is equivalent to close to 0.0648 ng/mL of endotoxin (considering that 1 EU/mL = 0.1 ng endotoxin/mL of solution [15]). This amount of LPS did not induce the expression of any inflammation marker in mice used in this study (data not shown).

Murine model of lung inflammation and bronchoalveolar lavages

A model of acute lung inflammation was performed as described previously [16] with some modifications. Briefly, C57 or *Lps del* mice were "whole body" nebulized with vehicle (saline), LPS (from *Escherichia coli,* serotype O55:B5), or S-RBD using glass cages with a filter on the top connected to a PVC tube, which was attached to the nebulizer Nebucor P-103 (México). For each nebulization protocol, a total volume of 5 mL of LPS or S-RBD solution was used, both at a concentration of 100 µg/mL. Then, four animals were placed per cage and the nebulization protocol was performed, which consisted of four nebulizations of 5 min each, alternate with 5 min of rest (without nebulization), with a total duration of 40 min. As a control, C57 and *Lps del* mice were nebulized, instead of LPS or S-RBD, with sterile saline or refolding buffer diluted in sterile saline to 5 mL (approx. 500–1000 µL of refolding buffer in 5 mL of sterile saline). In some experiments, different doses of Jacareubin (3.3 or 33 mg/kg), dexamethasone (20 mg/kg), or saline were administrated intraperitoneally to each C57 mouse 2 h before nebulization with S-RBD.

Once the nebulization protocol was finished, mice were sacrificed by CO_2 inhalation at different times (0, 0.5, 1,

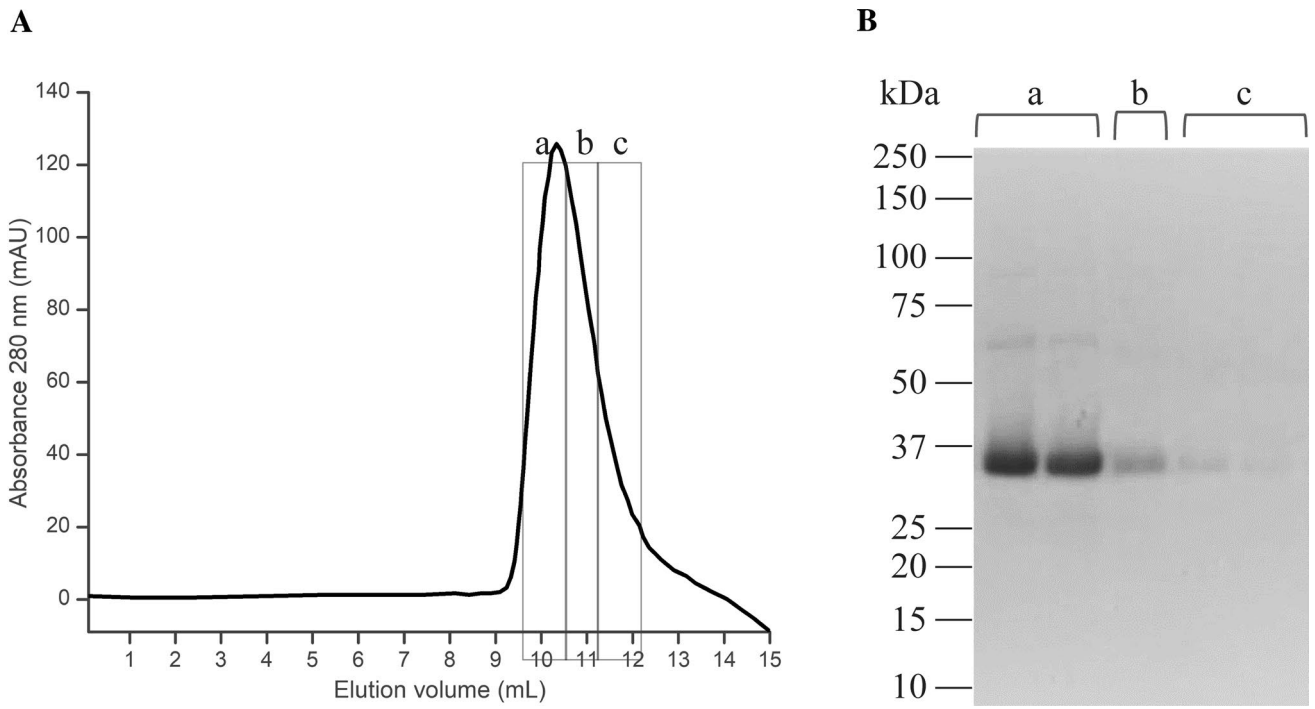

Fig. 2 Purification of the recombinant RBD domain of the Spike protein from SARS-CoV-2. **A** Gel filtration (last step of the purification) of the recombinant RBD showing the Abs_{280nm} chromatogram. **B** The fractions were analyzed by 8% SDS-PAGE showing a band corresponding to the predicted MW of the monomer, and some light bands corresponding to an SDS-resistant oligomers (fraction a). RBD: receptor-binding domain; SDS-PAGE: Sodium Dodecyl Sulphate–Polyacrylamide Gel Electrophoresis; MW: molecular weight; kDa: kilo Daltons

2, 4, 8, 12 y 24 h), where 0 h is immediately after nebulization (baseline). Subsequently, bronchoalveolar lavages (BALs) were performed as previously described [17]. In brief, a tracheotomy was performed, and the trachea was cannulated with a 22 G × 1″ catheter before exposing the thoracic cavity. Then, two separate 0.8-mL aliquots of sterile saline were slowly injected and aspirated, and this procedure was repeated two times. Approximately 1–1.2 mL of BAL were recovered per mouse and centrifugated at 10,000 rpm in a HERMLE Z-233 MK-2 centrifuge for 10 min at 4 °C. Finally, supernatants were obtained and stored at − 80 °C until assayed, and cell pellets were used for H&E staining as described in the next section.

Hematoxylin and eosin staining

Cell pellets (of three independent BALs obtained from three animals per condition) were resuspended in 500 µL of PBS-1X and placed on electrocharged slides for 15 min. Cells were then fixed in methanol for 5 min and stained with an H&E staining kit from Abcam (Cat. number: AB245880), according to the provider´s instructions. Images were acquired using an inverted optical microscope (Leica, Wetzlar, Germany) using the 10× and the 40× objectives. Magnification and cell counting was performed as follows: the full image obtained with the 40X objective was considered a "field" and it corresponds to an approximate area of 0.125 mm^2. Micrographs of at least three fields per slide were obtained with an EC3 camera (Leica) coupled to the microscope. The total number of cells per field at 40× was obtained analyzing each micrograph with the cell counting plugin of the free ImageJ software (NIH), and the results were expressed as the number of cells per field at 40×. Calibration bar was obtained using the software included with the EC3 Leica camera, the Leica Application Suite (LAS), version 3.2.0.

ELISA assay for TNF-α and IL-6 quantification

Concentrations of TNF-α and IL-6 were determined in 200 µL of each BAL using cytokine-specific enzyme-linked immunosorbent assay (ELISA) kits (PeproTech, USA. Cat. numbers: 900-K54 for TNF-α and 900-K50 for IL-6), according to the manufacturer's instructions. In each determination, a standard curve was used to calculate the concentration of TNF-α or IL-6 in picograms per milliliter (pg/mL) of BAL.

Data analysis

Data are expressed as mean ± SEM of at least four independent experiments, except when non-parametric tests were performed, in which case median and range are reported. Normal distribution of data was validated using Shapiro–Wilk test. Data from time courses of cytokine production and H&E cell counting experiments were analyzed by two-way ANOVA. When F achieved minimal statistical significance, the Dunnett or Tukey post hoc tests were used for multiple comparisons. Data generated of Jacareubin effects in the secretion of cytokines were analyzed using the Mann–Whitney test. Significant difference among experimental groups was set when $p < 0.05$.

Results

S-RBD triggers an intense TLR4 receptor-dependent lung inflammation in mice

The effect of the nebulization of RBD on lung inflammation of mice and its dependence on TLR4 receptor triggering was assessed. First, mice from the strains C57BL6/J (control, C57) and the TLR4-deficient (*Lps del*) were nebulized with bacterial LPS (100 µg/mL) as described by Skerrett et al. [16] and in the material and methods section. Then, bronchoalveolar lavages (BALs) were performed and the inflammatory response was evaluated by quantifying, by ELISA, the levels of TNF-α (for details, see materials and methods section). Results are presented in Figure S2. LPS treatment induced an increase in TNF-α concentrations in BALs of treated C57 mice (baseline: 91.5 ± 18.0 pg/mL; 2 h post-nebulization: 978.9 ± 57.8 pg/mL; Figure S2, gray bars). As expected, a diminished inflammatory response triggered by LPS was observed in *Lps del* mice compared to C57 mice, since no significant changes in TNF-α levels were found at any time evaluated (Figure S2, pink bars, RM-Two Way ANOVA; $F_{1,8} = 128.4$; $p < 0.001$; $n = 5$ animals per each condition). Predictably, no changes in TNF-α levels were observed when the LPS vehicle was nebulized (data not shown).

Next, C57 and *Lps del* mice were nebulized with distinct amounts of recombinant S-RBD (100 µg/mL, Fig. 3). A significant increase in TNF-α levels was observed at 2, 4, and 8 h post-nebulization with S-RBD, reaching the maximum value 4 h after nebulization (baseline: 151.4 ± 30.9 pg/mL; 4 h post-nebulization: 812.9 ± 29.2 pg/mL; Fig. 3A, gray bars). As observed with LPS-dependent TNF-α production, 12 and 24 h after S-RBD nebulization, TNF-α levels in BALs returned to baseline. Interestingly, TNF-α accumulation triggered by S-RBD was fully prevented in *Lps del* mice (Fig. 3A, pink bars, RM-Two Way ANOVA; $F_{1,8} = 211.8$; $p < 0.001$; $n = 5$ animals per each condition), As expected, no TNF-α production was observed in C57 or *Lps del* animals when the S-RBD vehicle (diluted refolding buffer, see material and methods section) was utilized for nebulization (results not shown).

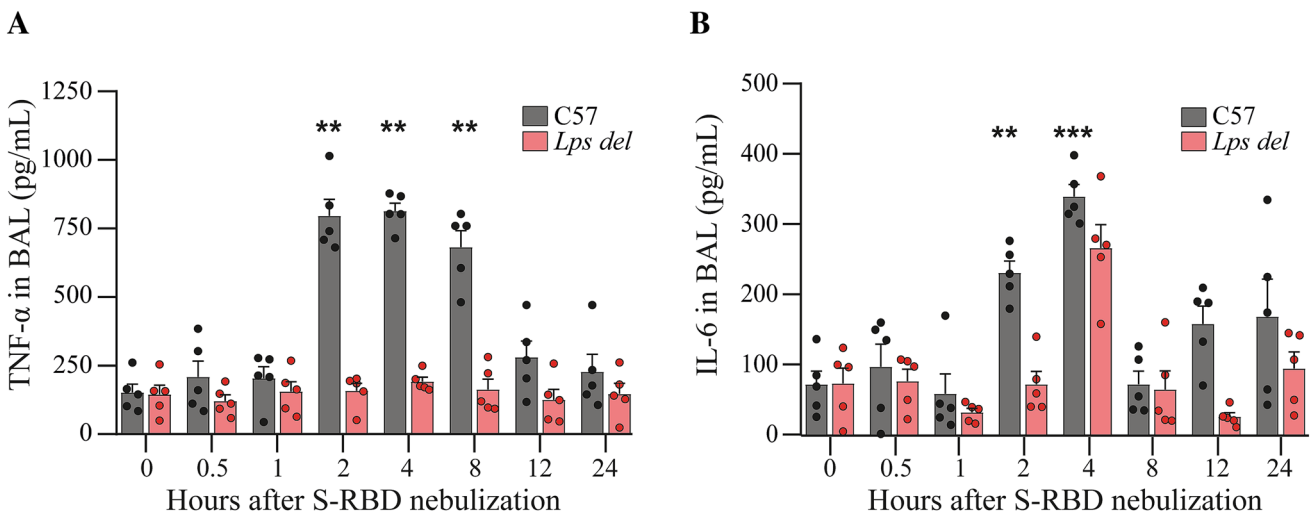

Fig. 3 S-RBD nebulization triggers an intense TLR4 receptor-dependent lung inflammation in mice. The effect of S-RBD nebulization on TNF-α **(A)** and IL-6 **(B)** secretion from C57 (gray bars) and *Lps del* (red bars) animals. TNF-α and IL-6 secretion was measured in BALs by ELISA at different time points post-nebulization. Data are presented as mean ± SEM. $^{**}p < 0.01$ and $^{***}p < 0.001$ vs 0 h post-nebulization using Two-way ANOVA and Dunnett post hoc test, $n = 5$ animals for each condition. S-RBD: RBD of the Spike protein; TNF-α: Tumor necrosis factor-alpha; IL-6: Interleukin 6; BALs: Bronchoalveolar lavages; ELISA: enzyme-linked immunosorbent assay

Since, together with TNF-α, IL-6 is an important component of the cytokine storm induced by SARS-CoV-2 infection (reviewed in [18]), we also evaluated the secretion of this cytokine in BALs of S-RBD-treated mice. As observed with TNF-α secretion, S-RBD elicited a rapid increase in the levels of IL-6 in BALs from C57 mice, reaching the maximal concentration 4 h after nebulization (baseline: 68.5 ± 19.2 pg/mL; 2 h post nebulization: 229.1 ± 16.9 pg/mL; 4 h post-nebulization: 338.9 ± 17.4 pg/mL). At longer times (8, 12 and 24 h post-nebulization), no significant changes in IL-6 values were found compared to baseline (Fig. 3B, gray bars). S-RBD nebulization in *Lps del* mice did not induce any significant change on IL-6 secretion at any time evaluated (Fig. 3B, pink bars, RM-Two Way ANOVA; $F_{1,8} = 31.4$; $p < 0.001$; n = 5 animals per each condition).

Additionally, cell infiltrates in retrieved BALs from C57 and *Lps del* mice treated with S-RBD were analyzed by H&E staining (Fig. 4). Representative photographs of the cells observed under the 10X and the 40× objectives are presented on Fig. 4A, whereas the number of cells detected in ten random fields observed under the 40× objective, in three independent BALs (see material and methods section), is shown in Fig. 4B. As observed, in C57 mice, S-RBD induces an increase in the number of recovered cells from BALs 2 h post nebulization (zero time post-nebulization: 30.0 ± 2.9 cells/field; 2 h post-nebulization: 58.8 ± 7.6 cells/field; $p < 0.001$). In contrast, in mice lacking TLR4, the number of infiltrating cells was not different between 0 and 2 h after nebulization with S-RBD (zero time after nebulization: 24.7 ± 2.3 cells/field; 2 h post-nebulization: 26.1 ± 1.9 cells/field; p = 0.996), showing a significant difference between mouse strains (Fig. 4B, RM-Two Way ANOVA; $F_{1,36} = 20.9$; $p < 0.001$; $n = 10$ fields per each condition). Taken together, these data demonstrate that S-RBD induces an acute lung inflammation through mechanisms involving TLR4 receptor activation and subsequent signaling.

Pretreatment with Jacareubin prevents lung inflammation triggered by S-RBD of the spike protein

Given that uncontrolled lung inflammation is probably one of the main causes of mortality in SARS-CoV-2 infection [19], we decided to evaluate the potential therapeutic effect of Jacareubin, a natural compound with previously demonstrated antioxidant and anti-inflammatory activity [10], on S-RBD-induced acute lung inflammation in C57 mice. Therefore, two different doses of Jacareubin (33 and 3.3 mg/kg) were ip administered 2 h before the nebulization with S-RBD, and TNF-α levels were measured in BALs 2 h after nebulization (for details, see materials and methods section). As expected, Jacareubin vehicle (saline) pretreatment did not prevent increased TNF-α secretion after nebulization with S-RBD (baseline: 208.9 (196.4) pg/mL; 2 h post-nebulization: 724.4 (228.3) pg/mL; Fig. 5 left panel, black symbols, Mann–Whitney test; $p = 0.0286$; $n = 4$ animals per time point). Pre-treatment with 3.3 or 33 mg/kg of Jacareubin prevented TNF-α increase induced by S-RBD nebulization (3.3 mg/kg, baseline: 155.3 (99.6) pg/mL; 2 h post-nebulization: 320.5 (319.1) pg/mL; Fig. 5 left panel,

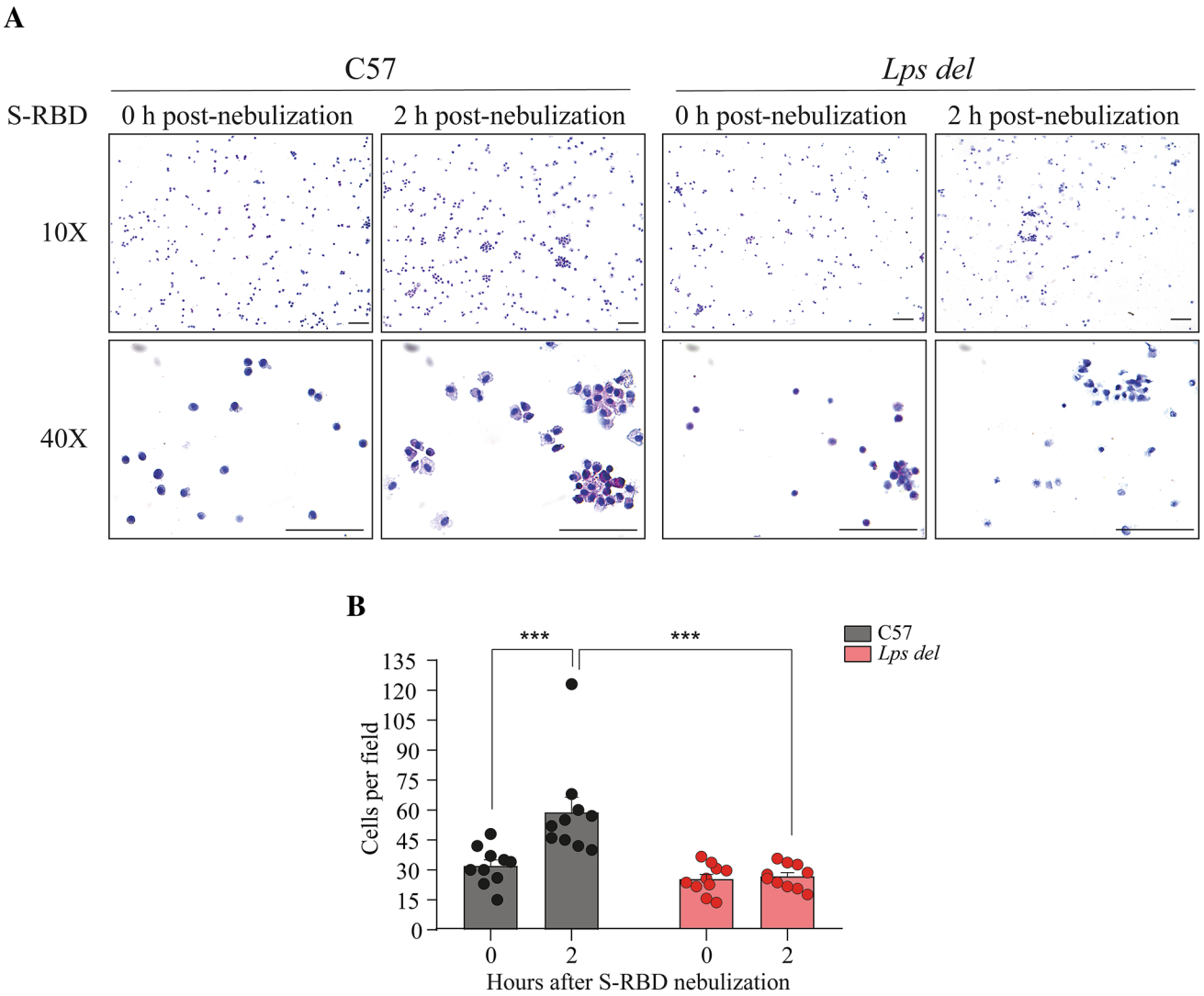

Fig. 4 H&E staining of cells pellets recovered from BALs. **A** Representative images of cells infiltrated in BALs from C57 mice (left panel) and *Lps del* mice (right panel) after 2 h post-nebulization with S-RBD. **B** Cell numbers detected in BALs from mice nebulized with S-RBD. Data were collected from at least three different random fields from slides with cells from independent BALs observed under a 40× objective (see Material and Methods section). Data are presented as mean ± SEM. ***$p < 0.001$ using Two-way ANOVA and Tukey post hoc test, $n = 10$ fields of at least 3 BALs per condition. Calibration bar = 100 µm. S-RBD: RBD of the Spike protein; BALs: Bronchoalveolar lavages

blue symbols, Mann–Whitney test; $p = 0.1143$; $n = 4$ animals per time point; and 33 mg/kg, baseline: 188.0 (141.8) pg/mL; 2 h: 243.0 (225.5) pg/mL; Fig. 5 left panel, purple symbols, Mann–Whitney test; $p = 0.6857$; $n = 4$ animals per time point). To compare the anti-inflammatory effect of Jacareubin with a potent well-known anti-inflammatory and immunosuppressant drug, a group of control mice was nebulized with dexamethasone (20 mg/kg) [20]. We found that, similar to Jacareubin, dexamethasone pre-treatment completely prevented RBD-induced TNF-α secretion 2 h after nebulization (Fig. 5 left panel, orange symbols). Finally, the effect of Jacareubin in S-RBD-induced IL-6 production was also evaluated. As observed in right panel of Fig. 5, pretreatment with Jacareubin (33 mg/kg) prevented IL-6 accumulation in BALs when measured at optimal time (zero time post-nebulization: 54.3 (70.6) pg/mL; 4 h post-nebulization: 83.8 (85.3) pg/mL; Fig. 5 right panel, purple symbols, Mann–Whitney test; $p = 0.3429$; $n = 4$ animals per time point).

Discussion

It is well accepted that ACE-2 mediates the entry of SARS-CoV- 2 into host cells via binding of the RBD domain-containing in its structural S protein [3]. However, in silico studies have revealed that S protein can interact with innate

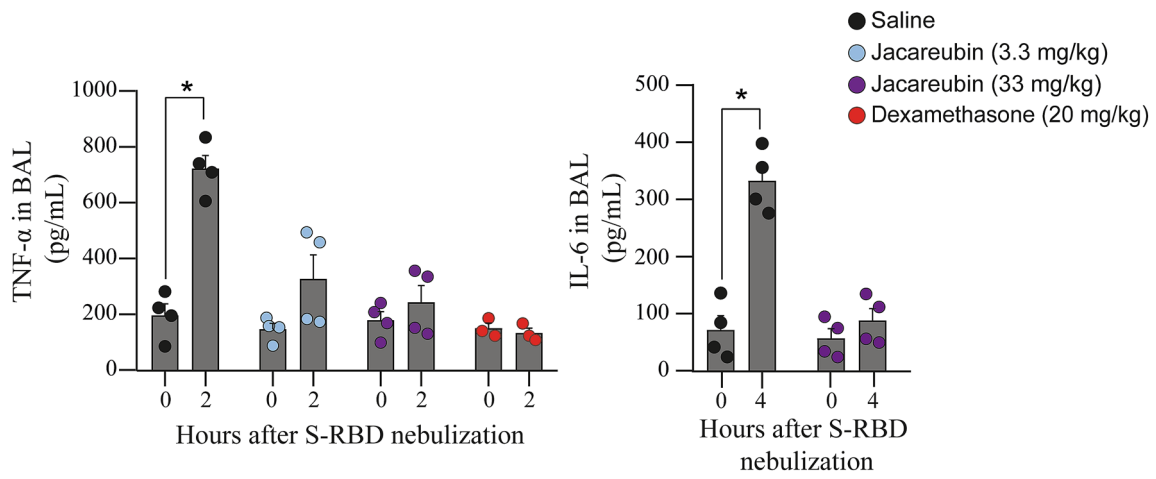

Fig. 5 Jacareubin inhibits S-RBD-induced TNF-α and IL-6 secretion in a murine model of lung inflammation. The effects of pretreatment with 3.3 or 33 mg/kg of Jacareubin or saline in TNF-α (left panel) and IL-6 (right panel) secretion are shown. After pretreatment (2 h), C57 mice were nebulized with S-RBD, and secretion of TNF-α and IL-6 in BALs was determined by ELISA at 0 and 2 h post-nebulization and 0 and 4 h post-nebulization, respectively. Dexamethasone pretreatment was used as a control. Comparisons were made between 0 and 2 h or 4 h post-nebulization of each experimental group. Data are presented as Median and range. $*p < 0.05$ vs 0 h post-nebulization using Mann–Whitney test, $n = 4$ animals for each condition. S-RBD: RBD of the Spike protein; TNF-α: Tumor necrosis factor-α; IL-6: Interleukin 6; BALs: Bronchoalveolar lavages

immune receptors such as Toll-like receptors (TLRs), raising the possibility that other receptors participate in the viral infection and inflammatory response [12] and S-RBD could be considered as a putative pathogen-associated molecular pattern (PAMP) recognized by TLR4 receptor. Here, we found that S-RBD nebulization triggers an intense lung inflammation in a TLR4-dependent manner, and this response is comparable to that induced by LPS. These results are in line with those found in silico and in cell cultures of innate immune cells, where it has been shown that S protein binds and activates TLR4 receptors and its signal transduction pathway. In monocytes and macrophages, S protein induces an increase in the secretion of TNF-α, IL-1β, and IL-6. Accordingly, that reported activity was blocked by the TLR4-specific inhibitor resatorvid or specific siRNAs and was absent in macrophages obtained from TLR4-deficient mice [12, 21–24]. Interestingly, TLR4 and its related signaling molecules were strongly overexpressed in alveolar macrophages after a challenge with the whole S protein [24]. In those studies, a direct interaction between TLR4 and the S protein of SARS-CoV-2 was suggested, although no specific epitope of S protein was identified as a ligand for the TLR4 receptor. The effect of monomeric S-RBD on the activation of immune cells with a possible participation of pattern recognition receptors (PRRs) has been documented. For example, primary dendritic cells derived from monocytes from healthy donors increased the expression of maturation markers in response to complete S protein or the purified S-RBD domain [25]. In that study, the secretion of IL-6, TNF-α, and IL-1β was also induced and the response to purified S-RBD domain was remarkably similar with that observed with LPS [25]. On the other hand, specific interaction of S-RBD domain with TLR4 has been previously reported [21]. Interestingly, S-RBD domain-dependent activation of TLR4 in THP-1 monocytes seems to require the formation of a trimeric aggregate, since the monomeric S-RBD did not induce cytokine production in those cells [21]. The discrepancy between results obtained from distinct in vivo and in vitro models of inflammation could be related to the formation of S-RBD aggregates in the protein preparations used, the aggregation of the protein due to the presence of lung mucins or discrete differences in the expression of PRRs and their co-receptors in each responsive cell. This interesting aspect should be further explored.

In the present study, we used the RBD domain of S protein and an in vivo model with *Lps del* mice, that present a deletion in the Lps locus and only the *TLR4* gene is absent in those animals [26]. Our data, using this animal model for the first time, strongly suggest that the S-RBD domain could be a ligand of the TLR4 receptor in the mice lung and adds to those studies that place this interaction as one of the main events that initiate the pulmonary inflammatory reaction in response to SARS-CoV-2 infection. However, further research should be conducted to discard the participation of other intermediate molecules.

Our study evaluated the inflammatory response by measuring cell infiltrate and TNF-α and IL-6 presence in BALs, through which we observed a local inflammation after S-RBD nebulization. This finding is relevant because SARS-CoV-2 infection occurs mainly in the lower respiratory tract

[27], and it is well known that respiratory failure is the primary cause of death by COVID-19 [28], an event that is accompanied by a cytokine storm that includes TNF-α, IL-1β, and IL-6, among other mediators. Several studies have evaluated the inflammatory response in bronchoalveolar fluids of COVID-19 patients. One of them was executed by Zhou and cols., who demonstrated by metatranscriptomic sequencing, that BALs of eight confirmed COVID-19 patients exhibited overexpression of proinflammatory genes compared to healthy controls, suggesting that infection by SARS-CoV-2 promotes a hyperproduction of inflammatory cytokines in the lung. Interestingly, several upregulated genes were associated with "interleukin" and "tumor necrosis factor" categories [9]. On the other hand, sepsis has been reported in almost all deceased patients, but the mechanism by which SARS-CoV-2 infection leads to viral sepsis remains unclear [29].

To date, approximately 5.6 million deceases have been reported worldwide despite the efforts to vaccinate the entire population (https://covid19.who.int/ accessed on 31 January 2022) [30], making the identification of new accessible compounds for COVID-19 treatment a very important area on the search of therapeutic strategies. We evaluated the potential therapeutic effect of Jacareubin, a natural compound with antioxidant and anti-inflammatory properties whose safety and low toxicity, at least at the dose used in this study, have been tested both in vivo and in vitro [31]. We previously demonstrated that Jacareubin inhibits FcεRI-induced degranulation of cultured mast cells (MCs) by inhibiting the production of ROS required to activate calcium channels and subsequent activation of MCs. Moreover, it was demonstrated that Jacareubin hinders local inflammatory reactions in vivo dependent on MCs and phagocytes [10]. Here, we showed that Jacareubin completely blocked the over-release of TNF-α and IL-6 in the lungs, triggered by S-RBD nebulization.

This finding is in line with those obtained in vitro utilizing compounds such as palmitoylethanolamide and cannabidiol, which have shown anti-inflammatory effects in response to stimulation of cultured cells with the S protein of SARS-CoV-2 [24, 32]. Our results (performed with an in vivo model of lung inflammation), suggests that Jacareubin is a natural product able to prevent S-RBD-induced lung damage. If Jacareubin can improve survival after SARS-CoV-2 viral infection in murine or other in vivo models, remains as an unexplored aspect on the actions of this compound. Identification of potential therapeutic agents against COVID-19 is especially relevant in a context where new SARS-CoV-2 variants are regularly found [33, 34]. In that sense, additional strategies, besides vaccines, are required for improving the prognosis of severe forms of COVID-19.

Although this work provides important new insights regarding the identification of the PRRs involved in S-RBD recognition and the characterization of potentially useful natural compounds to treat COVID-19, we are aware of the limitations of the study, such as the use of mice derived from one single strain (C57BL6/J) and the relatively small sample size utilized. Also, effects of Jacareubin on other pro-inflammatory parameters associated to COVID-19 (such as the production of other cytokines or reactive oxygen species, ROS) remain to be evaluated. Current studies in our laboratories are now being conducted to evaluate those and other immunological parameters in response to S-RBD in mice and the effects of Jacareubin. Nevertheless, this work provides new information that improves the understanding of the molecular pathophysiology of COVID-19 and potentially therapeutic natural agents.

In summary, our results strongly suggest that S-RBD could interact with TLR4 receptors to induce a rapid increase in the number of infiltrated cells and TNF-α and IL-6 levels in the lung. Also, our data show that the natural xanthone Jacareubin is a novel anti-inflammatory compound that may have potential therapeutic applications to control the excessive inflammatory response observed in COVID-19 and illustrate the importance of biodiversity in drug discovery.

Supplementary Information The online version contains supplementary material available at https://doi.org/10.1007/s43440-022-00398-5.

Author contributions DSV.: conceptualization, methodology, validation, investigation, formal analysis, and writing-original draft. EMR, DRV, DIZV, and JGFV.: production and purification of the Spike protein RBD domain. JICA and RRC.: Jacareubin isolation, chemical characterization, and purity analysis. CGE.: conceptualization, resources, project administration, and writing-review & editing.

Funding This work was supported by funds from the Agencia Mexicana de Cooperación Internacional para el Desarrollo (AMEXCID) of the Secretaría de Relaciones Exteriores (SRE), Project AMEXCID_2020-3 to E. M. R. Also, funds were provided by Consejo Nacional de Ciencia y Tecnología (Conacyt) Grants Conacyt CB2017-2018 A1-S-10743 and Apoyo para proyectos de investigación científica, desarrollo tecnológico e innovación en salud ante la contingencia por COVID-19 311835 to E.M.R.; Grant Conacyt CF-2019–51488 to C.G.E. Other funds were obtained from the Secretaría de Educación Pública (SEP) and Cinvestav (Grant SEP-Cinvestav 2018:1 to E.M.R.) and Gobierno del Estado de Hidalgo (Proyectos Sincrotrón 20201120 and 20201039 to E.M.R.). J.G.F.V., D. R. V., and D. I. Z. V. received a predoctoral fellowship from Conacyt. D.R.V. is a student of the Nanociencias and Nanotecnología PhD program at Cinvestav. D.S-V. received a PhD scholarship (No. 781556) from Conacyt. J.I.C-A. received a postdoctoral fellowship from DGAPA-UNAM. Authors wish to thank Juan Javier López-Guerrero (Departamento de Farmacobiología, Cinvestav) for technical assistance in bronchoalveolar lavages technique implementation. We also thank Beatriz Quiroz-Vázquez and Javier Pérez-Flores (Instituto de Química-UNAM) for the NMR and EM determinations, together with Dr. Jorge Fernández Hernández, Víctor Manuel García Gómez, Ricardo Gaxiola Centeno, María Antonieta López-López, and Benjamín E. Chávez-Álvarez for assistance in maintaining the colonies of mice used in this study.

Declarations

Conflict of interest D. R. V., J. G. F. V., D. I. Z. V., and E. M. R. declare that they are in the process of filing a patent application including the sequence, the methodology of purification, and refolding of the S-RBD protein. The rest of the authors declare that they have no conflict of interest regarding the work submitted.

Data availability Datasets generated during and/or analyzed during the current study are included in this published article (and its supplementary information files).

References

1. Koch J, Uckeley ZM, Lozach P. SARS-CoV-2 variants as super cell fusers: cause or consequence of COVID-19 severity? EMBO J [Internet]. 2021;15: e110041.
2. Wang M-Y, Zhao R, Gao L-J, Gao X-F, Wang D-P, Cao J-M. SARS-CoV-2: Structure, Biology, and Structure-Based Therapeutics Development. Front Cell Infect Microbiol [Internet]. 2020;10(November):587269.
3. Zhao Y, Zhao Z, Wang Y, Zhou Y, Ma Y, Zuo W. Single-Cell RNA expression profiling of ACE2, the receptor of SARS-CoV-2. Am J Respir Crit Care Med. 2020;202(5):756–9.
4. Zou X, Chen K, Zou J, Han P, Hao J, Han Z. Single-cell RNA-seq data analysis on the receptor ACE2 expression reveals the potential risk of different human organs vulnerable to 2019-nCoV infection. Front Med. 2020;14(2):185–92.
5. Chen Y, Guo Y, Pan Y, Zhao ZJ. Structure analysis of the receptor binding of 2019-nCoV. Biochem Biophys Res Commun. 2020;525(1):135–40.
6. Hu B, Huang S, Yin L. The cytokine storm and COVID-19. J Med Virol. 2021;93(1):250–6.
7. Hussman JP. Cellular and molecular pathways of covid-19 and potential points of therapeutic intervention. Front Pharmacol. 2020;11(July):1–17.
8. Qin C, Zhou L, Hu Z, Zhang S, Yang S, Tao Y, et al. Dysregulation of immune response in patients with coronavirus 2019 (COVID-19) in Wuhan. China Clin Infect Dis. 2020;71(15):762–8.
9. Zhou Z, Ren L, Zhang L, Jin Q, Li M, Wang J. heightened innate immune responses in the respiratory tract of COVID-19 patients ll ll short article heightened innate immune responses in the respiratory tract of COVID-19 patients. Cell Host Microbe. 2020;27(6):883–90.
10. Castillo-Arellano JI, Guzmán-Gutiérrez SL, Ibarra-Sánchez A, Hernández-Ortega S, Nieto-Camacho A, Medina-Campos ON, et al. Jacareubin inhibits FcεRI-induced extracellular calcium entry and production of reactive oxygen species. Biochem Pharmacol. 2018;154:344–56. https://doi.org/10.1016/j.bcp.2018.05.002.
11. Wan Y, Shang J, Graham R, Baric RS, Li F. Receptor recognition by the novel coronavirus from wuhan: an analysis based on decade-long structural studies of sars coronavirus. J Virol. 2020;94(7):1–9.
12. Choudhury A, Mukherjee S. In silico studies on the comparative characterization of the interactions of SARS-CoV-2 spike glycoprotein with ACE-2 receptor homologs and human TLRs. J Med Virol. 2020;92(10):2105–13.
13. Dodd RB, Allen MD, Brown SE, Sanderson CM, Duncan LM, Lehner PJ, et al. Solution structure of the Kaposi's sarcoma-associated herpesvirus K3 N-terminal domain reveals a Novel E2-binding C4HC3-type RING domain. J Biol Chem. 2004;279(51):53840–7.
14. Lartey NL, Valle-Reyes S, Vargas-Robles H, Jiménez-Camacho KE, Guerrero-Fonseca IM, Castellanos-Martínez R, et al. ADAM17/MMP inhibition prevents neutrophilia and lung injury in a mouse model of COVID-19. J Leukoc Biol. 2022;111(6):1147–58. https://doi.org/10.1002/JLB.3COVA0421-195RR (**Epub 2021 Nov 26**).
15. What is Endotoxin-GenScript.Page: https://www.genscript.com/endotoxin-kits.html. Accesed 15 July 2022.
16. Skerrett SJ, Liggitt HD, Hajjar AM, Ernst RK, Miller SI, Wilson CB. Respiratory epithelial cells regulate lung inflammation in response to inhaled endotoxin. Am J Physiol-Lung Cell Mol Physiol. 2004;287(1):L143–52. https://doi.org/10.1152/ajplung.00030.2004 (**Epub 2004 Mar 26**).
17. Sun F, Xiao G, Qu Z. Murine bronchoalveolar lavage. Bio-Protoc. 2017;7(10):1–7.
18. Mohseni Afshar Z, Barary M, Babazadeh A, Tavakoli Pirzaman A, Hosseinzadeh R, Alijanpour A, et al. The role of cytokines and their antagonists in the treatment of COVID-19 patients. Rev Med Virol [Internet]. 2022;27(May): e2372.
19. Fu Y, Cheng Y, Wu Y. Understanding SARS-CoV-2-Mediated Inflammatory Responses: From Mechanisms to Potential Therapeutic Tools. Virol Sin. 2020;35(3):266–71. https://doi.org/10.1007/s12250-020-00207-4.
20. Zuckerman SH, Bendele AM. Regulation of serum tumor necrosis factor in glucocorticoid-sensitive and -resistant rodent endotoxin shock models. Infect Immun. 1989;57(10):3009–13.
21. Zhao Y, Kuang M, Li J, Zhu L, Jia Z, Guo X, et al. SARS-CoV-2 spike protein interacts with and activates TLR41. Cell Res. 2021;31(7):818–20.
22. Shirato K, Kizaki T. SARS-CoV-2 spike protein S1 subunit induces pro-inflammatory responses via toll-like receptor 4 signaling in murine and human macrophages. Heliyon. 2021;7(2):e06187.
23. Jung HE, Lee HK. Current understanding of the innate control of toll-like receptors in response to SARS-CoV-2 infection. Viruses. 2021;13(11):2132.
24. Del Re A, Corpetti C, Pesce M, Seguella L, Steardo L, Palenca I, et al. Ultramicronized palmitoylethanolamide inhibits NLRP3 inflammasome expression and pro-inflammatory response activated by SARS-CoV-2 spike protein in cultured murine alveolar macrophages. Metabolites. 2021;11(9):592.
25. Barreda D, Santiago C, Rodríguez JR, Rodríguez JF, Casasnovas JM, Mérida I, et al. SARS-CoV-2 Spike protein and its receptor binding domain promote a proinflammatory activation profile on human dendritic cells. Cells. 2021;10(12):3279.
26. Poltorak A, Smirnova I, Clisch R, Beutler B. Limits of a deletion spanning Tlr4 in C57BL/10ScCr mice. J Endotoxin Res. 2000;6(1):51–6.
27. Zhou Z, Ren L, Zhang L, Zhong J, Xiao Y, Jia Z, et al. Heightened innate immune responses in the respiratory tract of COVID-19 patients. Cell Host Microbe. 2020;27(6):883-890.e2.
28. Huang C, Wang Y, Li X, Ren L, Zhao J, Hu Y, et al. Clinical features of patients infected with 2019 novel coronavirus in Wuhan. China Lancet. 2020;395(10223):497–506.
29. López-Collazo E, Avendaño-Ortiz J, Martín-Quirós A, Aguirre LA. Immune response and COVID-19: a mirror image of sepsis. Int J Biol Sci. 2020;16(14):2479–89.
30. World Health Organization (2021) WHO Coronavirus (COVID-19) Dashboard. WHO Coronavirus (COVID-19) Dashboard With Vaccination Data [Internet]. Who. p. 1–5. Page: https://covid19.who.int/. Accesed 31 Jan 2022.
31. García-Niño WR, Estrada-Muñiz E, Valverde M, Reyes-Chilpa R, Vega L. Cytogenetic effects of jacareubin from calophyllum brasiliense on human peripheral blood mononucleated cells in vitro and on mouse polychromatic erythrocytes in vivo. Toxicol Appl Pharmacol. 2017;335:6–15.

32. Corpetti C, Del Re A, Seguella L, Palenca I, Rurgo S, De Conno B, et al. Cannabidiol inhibits SARS-Cov-2 spike (S) protein-induced cytotoxicity and inflammation through a PPARγ-dependent TLR4/NLRP3/Caspase-1 signaling suppression in Caco-2 cell line. Phyther Res. 2021;2(June):1–11.
33. Yang L, Li J, Guo S, Hou C, Liao C, Shi L, et al. SARS-CoV-2 Variants, RBD mutations binding affinity, and antibody escape. J Mol Sci. 2021;22(22):12114. https://doi.org/10.3390/ijms222212114.
34. Hayawi K, Shahriar S, Serhani MA, Alashwal H, Masud MM. Vaccine versus Variants (3Vs): Are the COVID-19 Vaccines Effective against the Variants? A Systematic Review. Vaccines. 2021;9(11):1305.